EREM 79/4
Journal of Environmental Research, Engineering and Management
Vol. 79 / No. 4 / 2023
pp. 112–123
DOI 10.5755/j01.erem.79.4.32708

Adsorption of Cu(II) from Aqueous Solution on Sonicated Activated Carbon Prepared from *Arenga Pinnata Merr* Fruit Shell Waste: Isotherm, Kinetic and Thermodynamic Studies

Received 2022/11 | Accepted after revisions 2023/08

https://doi.org/10.5755/j01.erem.79.4.32708

Adsorption of Cu(II) from Aqueous Solution on Sonicated Activated Carbon Prepared from *Arenga Pinnata Merr* Fruit Shell Waste: Isotherm, Kinetic and Thermodynamic Studies

Syahiddin Dahlan Said[1], Abrar Muslim[1]*, Azwar Yahya[1], Nasrullah Razali[1], Qodri Yudit Angesta[1], Irmayani[2], Tony Hadibarata[3], Atikah Kadri[4]

[1] Department of Chemical Engineering, Faculty of Engineering, Universitas Syiah Kuala, Indonesia

[2] Department of Industrial Engineering, Faculty of Engineering, Universitas Teuku Umar, Indonesia

[3] Department of Environmental Engineering, Faculty of Engineering and Science, Curtin University Malaysia, Malaysia

[4] School of Chemical Engineering, College of Engineering, Universiti Teknologi MARA (UiTM), Malaysia

***Corresponding author:** abrar.muslim@usk.ac.id

Adsorption of Cu(II) from aqueous solution on the activated carbon (AC) prepared from *Arenga pinnata Merr* fruit shell (APMFS) waste with the assistance of ultrasound was evaluated by conducting batch mode experiments. As a result, KOH activation using 40 kHz of ultrasound restructured active binding sites and produced more pores on the APMFS-AC according to FT-IR and SEM analyses, respectively. Increasing the sonication time from 45 min to 135 min increased the adsorption capacity from 6.535 mg/g to 7.042 mg/g, respectively, at the initial Cu(II) concentration of 257.213 mg/L, 27°C and pH 5. With an increment of the adsorption temperature to 45°C, it increased the adsorption capacity up to 11.765 mg/g. The investigation on the independent variables showed the optimum conditions of adsorption which were 257.213 mg/L of the initial Cu(II) concentration, 60 min of contact time, pH 5 and 45°C using 135 min of sonicated APMFS-AC. The Cu(II) adsorption isotherm was fitted with the Langmuir model at the optimum condition. The Langmuir mono-layer adsorption capacity obtained was 11.765 mg/g with

the BET saturation capacity, and the total pore volume values were 13.029 mg/g and 3.987 L/mg, respectively. The Cu(II) adsorption followed the pseudo second-order kinetics model with the adsorption rate 0.473 g/mg.min. Thermodynamic parameters of enthalpy change (ΔH^0, 27.035 kJ/mol), Gibbs free energy (ΔG^0, 7.292 kJ/mol), entropy change (ΔS^0, 0.062 kJ/mol.K), and activation energy (E, 22.637 kJ/mol) were determined. These results confirmed that endothermic, spontaneous and chemical adsorption took place.

Keywords: *Arenga pinnata Merr*, activated carbon, ultrasound, isotherm, kinetics, thermodynamic.

Introduction

Heavy metals are non-biodegradable pollutants that may accumulate in human and animal bodies. The pollutants of heavy metals may be released uncontrollably from mining, metallurgical, petroleum refining processes (Srivastava and Majumder, 2008) and agricultural industries (Bala et al., 2008; Yan-Biao et al., 2013; Dimple, 2014). Among heavy metals, Cu(II) is found in industrial wastewater as a harmful pollutant (Minamisawa et al., 2004). It may cause disorders of the tissues, systems and organs of the human body (Theophanides and Anastassopoulou, 2002; Carl et al., 2003). Hence, removing Cu(II) from wastewater before discharging to the environment is necessary.

Activated carbon from low cost lignocellulosic material has been proposed to meet the global activated carbon consumption. Activated carbon consumption is growing gradually at an annual growth rate of + 0.6% by 2027, and it has been projected to achieve an amount of 4.5M tons of market volume by the end of 2030 (Mordor Intelligence, 2022). Lignocellulosic residue-based activated carbon has been tested for the Cu(II) adsorption using hazelnut husks and shell (Imamoglu and Tekir, 2008; Demirbas et al., 2009), pecan shells (Klasson et al., 2009), cassava peel (Moreno-Pirajan and Giraldo, 2010), corn cob (Milenković et al., 2013), biomass gasification residue (Runtti et al., 2014), Tunisian date stones (Bouhamed et al., 2012), and Australian pine cones (Muslim, 2017). However, activated carbon prepared from *Arenga pinnata Merr* fruit shell (APMFS) waste has not been developed and tested, especially for Cu(II) adsorption. Meanwhile, the APMFS soaked using nitric acid has been investigated as a biosorbent for the adsorption of Cr(II), Cr(IV) and Zn(II), but the biosorbent capacity has been found to be in a low range of 0.28–0.58 mg/g (Zein et al., 2014).

The APMFS waste could be an appropriate material for activated carbon production because of the increase in tree plantations across Asia for foods, bioethanol and composites (Ishak et al., 2013). Several chemicals, adsorption conditions and activation methods for activated carbon production have been reviewed (Kurniawan et al., 2006). Microwave radiation methods for preparing activated carbon (Dehdashti et al., 2010; Chen et al., 2011; Hesas et al., 2013) and agitation using ultrasound for adsorption (Milenković et al., 2013; Gupta and Gogate, 2016) have been proposed to increase Cu(II) adsorption capacity. Sonication of sludge for 15 min at 20 kHz using an ultrasonic probe can restructure the active binding sites of the adsorbent and increase the Cu(II) adsorption capacity (Commenges-Bernole and Marguerie, 2009). Ultrasonic assistance had not been applied in the production of adsorbent from the APMFS waste (Zein et al., 2014).

The main objective of this study was to prepare activated carbon from the APMFS waste. The novelty of this study was the production of activated carbon from the APMFS waste by carbonation at 800°C, and the APMFS waste carbon was activated using KOH with the assistance of ultrasound at 40 kHz. The effects of initial concentration of Cu(II), contact time, sonification (US) time, adsorption temperature and pH on the activated carbon (APMFS-AC) capacity were examined. The structural characterization of the APMFS waste, APMFS carbon and the APMFS-AC was performed by FT-IR and SEM analyses in order to provide relations between the analyses and Cu(II) adsorption capacity of the APMFS-AC. The constants of isotherm, kinetic and thermodynamic adsorption were determined by fitting the experimental data to the related mathematical models.

Materials and Methods

Materials

The APMFS waste was collected from the fruit processed in the Pucok village, Aceh Province, in the production of jelly endosperms called 'kolang kaleng'. Jelly

endosperms are generally removed from young and green fruits after boiling them for 3 h. Meanwhile, the wet fruit shell waste is often thrown away and dumped until it forms a pile and rots threatening the environment. To prepare the APMFS-AC raw material, 2 kg of the APMFS waste was cleaned and rinsed using tap water, and then dried in an oven drier (Memmert, Western Germany) at 115°C (± 1°C) for 12 h to remove water. The stock Cu(II) aqueous solution of 250 mg/L was made using $CuSO_4.5H_2O$ (99%, Aldrich), and it was analyzed by Atomic Absorption Spectrophotometer (AAS) (Shimadzu AA 6300, Japan) at wavelengths of 389.95 using a pre-mixed burner air-acetylene flame.

Activated carbon preparation and characterization

The same carbonation procedure of Australian pine cones (Muslim, 2017) was taken into account for carbonation of the dried APMFS waste. It was milled to powder, and 1 kg of the powder was carbonized in a furnace (Nabertherm, Germany) at 800°C (± 1°C) for 3 h. The APMFS waste carbon was milled at the room temperature using a ball mill, and sieved into 60–75 mesh. Then 50 g of the APMFS waste carbon was activated using 150 mL KOH at a concentration of 0.5 M (97% pure from Merk) for 136-min at 27°C in 250-mL beaker glass placed in an ultrasonic bath (Bransonic 8510, 40 kHz, made in USA). It was stirred at 75 rpm for 1 min at the beginning, and followed by a 45-min sonication. Then, the APMFS-AC was washed using distilled water to reach a neutral pH (7 ± 0.5). The APMFS-AC and water were separated using a vacuum filter. This activation procedure was repeated for 50 g of the APMFS waste carbon with a 135-min sonication. The APMFS-AC with different sonication times was dried separately in the oven drier (Memmert, Western Germany) at 120°C (± 1°C) for 4 h to remove water. All APMFS-AC was stored in sealed bottles.

FT-IR analysis using a spectrophotometer (IR Prestige 21-Shimadzu, Japan) was conducted with the spectra ranging from 400 to 4000 cm^{-1} to obtain the chemical functional groups of adsorbents at the spectra of 400–4000 cm^{-1}. The sample transmission spectra were obtained using KBr pellets at a 0.1% sample as mentioned in the previous study (Muslim, 2016). To view surface micrographs of the APMFS waste-based adsorbent, SEM at 500VA, 50/60Hz of 1 phase (TM3000-Hitachi, Japan) was used. The total pore volume and saturation capacity could be more efficiently determined by the Brunauer-Emmett-Teller (BET) analysis. However, the service for BET analysis is not available at Syiah Kuala Unversity. Therefore, the total pore volume and saturation capacity were determined using the BET model (Foo and Hameed, 2010).

Experiments of Cu(II) adsorption

Adsorption tests in a batch mode were run in 100-mL Erlenmeyer flasks consisting of 1 g of the APMFS-AC and Cu(II) solutions of 100 mL. All the adsorption tests were conducted at 100-rpm stirring speed and atmospheric pressure (1 atm). The Cu(II) adsorption capacity, denoted as q by the APMFS-AC over independent variables, was examined. These were the contact time (0–80 min), initial concentration of Cu(II) in aqueous solution, denoted as C_0 (18.372–257.213 mg/L), the pH of Cu(II) solutions (3–7), adsorption temperature (27–45°C) and sonication time of chemical activation (45–135 min). The wide range of C_0 under acidic conditions was applied to obtain maximum q (Kurniawan et al., 2006). To control the adsorption temperature, an Alpha Immersion thermostat (230V, 50/60 Hz, Germany) and a bath for the thermostat (6L, Makrolon) installed with an internal circulation pipe were used. The Erlenmeyer flask containing the solution, activated carbon and magnetic bar was put in the bath. The bath installed with the thermostat was placed on a magnetic stirrer.

The same procedure of Cu(II) adsorption by the activated carbon of Australian pine cones (Muslim, 2017) was used for the adsorption tests. The initial pH was adjusted with HCl or NaOH (Pandian et al., 2021) (99.8%, Gatt-Koller) by dropping it at a concentration of 0.01–1 M, and measured using a portable PHYWE pH Meter (Cobra4, Germany). The Cu(II) adsorption isotherm, kinetic and thermodynamic studies were conducted using the experimental data and previous procedure (Muslim et al., 2022), and the values of the parameters were obtained using related equations.

Results and Discussion

The functional groups of the APMFS waste powder and the APMFS-AC

The dried APMFS waste powder contained more bands compared with APMFS carbon and the APMFS-AC with 45-min and 135-min sonication as shown in *Fig. 1*. A band at 3699–3776 cm^{-1} with the peak at 3722 cm^{-1} is

Fig. 1. *The FT-IR spectra of the dried APMFS waste powder, the APMFS carbon, the APMFS-AC with the 45-min sonication, and the APMFS-AC with the 135-min sonication*

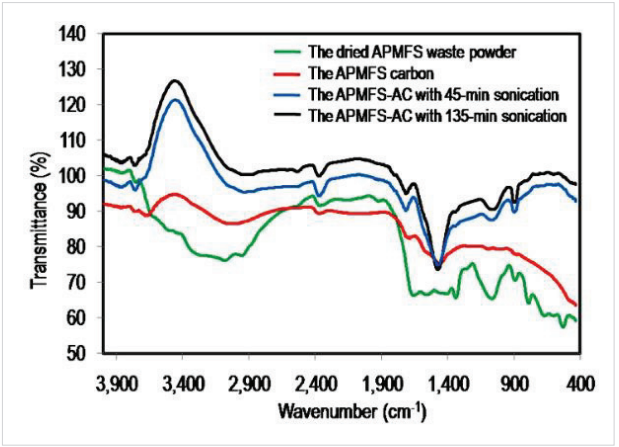

assigned to hydroxyl groups of non-hydrogen bonded O–H stretching (Yang and Lua, 2003). An increase of transmittances indicated that pyrolysis reduced hydroxyl groups, and 0.5 M KOH activation with ultrasound restructured O–H active binding sites of the APMFS carbon. The same trend was also reported in a previous study (Commenges-Bernole and Marguerie, 2009). Meanwhile, the hydroxyl and amide group of O–H and N–H stretching at 3300–3500 cm^{-1} (Hesas et al., 2013; Zein et al., 2014) in the dried APMFS waste powder was completely removed as a result of pyrolysis and KOH activation. Chemical activation using an ultrasound bath also removed the C–H stretch of aromatics with the band at 3000–3100 cm^{-1} and the peak at 3055 cm^{-1}, and the C–H stretch of alkenes with the band at 2850–3000 cm^{-1} and the peak at 2930 cm^{-1} (Zein et al., 2014).

A band at 1570–1700 cm^{-1} with the peak at 1653 cm^{-1} in the dried APMFS waste powder is attributed to the C=O stretching of ketones (Chakravarty et al., 2010), and it increased due to the sonication. Another weak band at 1286–1400 cm^{-1} with the peak at 1317 cm^{-1} and the transmittance of 62.17% in the dried APMFS waste represents the C–H asymmetrical and symmetrical stretching (Hesas et al., 2013). This band is absent in the APMFS-AC. The strongest and wide new band at 1371–1548 cm^{-1} with the peak at 1456 cm^{-1} assigned to the C=O stretching of amides (Chakravarty et al., 2010) appeared in the APMFS-AC with the transmittance of 73.06%, as seen in *Fig. 1*. A band at 1000–1260 cm^{-1} ascribed to the C–O stretching of carboxylic acids (Chakravarty et al., 2010) with the peak at 1033 cm^{-1} in the dried APMFS waste powder was almost completely removed by the pyrolysis, and it was restructured by the ultrasound. The last bands in the dried APMFS waste powder were associated with the C–C stretching at 400–700 cm^{-1} of carboxylic acids and ester (Hesas et al., 2013) with the peaks at 650 cm^{-1}, 582 cm^{-1} and 516 cm^{-1}. The bands were absent in the APMFS carbon and the APMFS-AC indicating that pyrolysis and sonication removed a significant amount of carboxylic acids and ester.

The surface morphology of dried APMFS waste powder and the dried APMFS-AC

As can be observed in *Fig. 2(a)*, irregular pores were shown on the dried APMFS waste powder, which were also reported for different raw materials of adsorbent in the past studies (Zengin et al., 2012; Muslim et al., 2015). Meanwhile, the pores were opened in the APMFS-AC showing the effect of pyrolysis, KOH activation, and ultrasound assistance.

Fig. 2. *The SEM micrographs of the surface of (a) the dried APMFS waster powder, (b) the APMFS-AC with the 45-min sonication, (c) the APMFS-AC with the 135-min sonication*

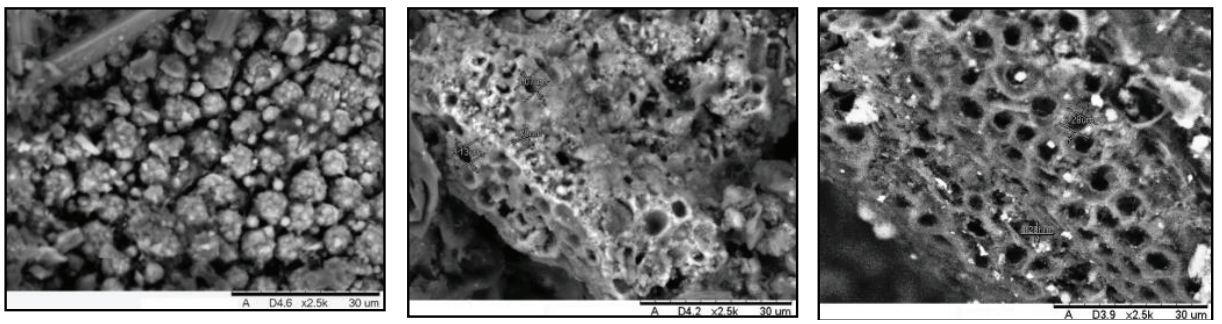

a *b* *c*

Effect of contact time on the *q*

In general, the heavy metals adsorption capacity of adsorbent increases exponentially over contact time (Wong et al., 2003; Mengistie et al., 2008). The equilibrium contact time, denoted as t_e, was at 120 min for tartaric acid activated rice husk (Wong et al., 2003), 20 min and 3 h for the Areca catechu heartwood AC (Chakravarty et al., 2010) and Militia ferruginea leaves AC (Mengistie et al., 2008), respectively. As can be seen in *Fig. 3(a)*, the *q* increased by 3.01 mg/g and 5.11 mg/g at a 10-min contact time at 27°C for adsorption using the APMFS-AC 45-min US and the APMFS-AC 135-min US, respectively, for the condition of C_0 being 257.213 mg/L at pH 5. It increased by 7.09 mg/g at 45°C using the APMFS-AC 135-min US. Then, it gradually increased until reaching the maximum adsorption capacity which was 6.58 mg/g, 7.14 mg/g and 8.90 mg/g at 40 min, and decreased a bit to 6.13 mg/g, 6.58 mg/g and 8.21 mg/g at 60 min for the three conditions, respectively. In this stage, the driving force for the diffusion of the adsorbate onto the adsorbent is becoming smaller and smaller due to the decrease of the mass of the adsorbate in solution and on the adsorbent (Medhi et al., 2020). Overall, it exponentially increased over contact time, and the t_e chosen was 60 min.

Effect of the C_0 on the *q*

Various trends of adsorbent capacity over the C_0 were reported. The *q* trends could be non-linear (Muslim et al., 2015), almost linear (Chakravarty et al., 2010), and exponential trends (Tseng and Tseng, 2005). *Fig. 3(b)* shows the *q* at pH 5. As shown by the top plot, the *q* by the APMFS-AC with the 135-min sonication at 45°C increased from 1.54 mg/g to 9.32 mg/g for the increase in the C_0 from 18.37 mg/L to 110.23 mg/L, and then it increased very slowly to 9.87 mg/g and 9.98 mg/g at the C_0 of 183.72 mg/L and 257.21 mg/L, respectively. Meanwhile, it decreased very slowly from 7.01 mg/g at 110.23 mg/L to 7.14 mg/g and 6.58 mg/g at 183.72 mg/L and 257.21 mg/L, respectively, at 27°C. The same trend is also shown by the APMFS-AC with the 45-min sonication. More diffusion of Cu(II) onto the surface and pores of the APMFS-AC should be caused by the more initial Cu(II) presented in the solution. The *q* can increase with the increase in the C_0. However, the *q* should be unchanging at the saturation even in case of the C_0 changing (Liu et al., 2014). Therefore, the increase in the *q* over the C_0 followed an exponential trend (Marlina et al., 2020).

Fig. 3. *The q of the APMFS-AC over (a) contact time (b) C_0 and (c) pH*

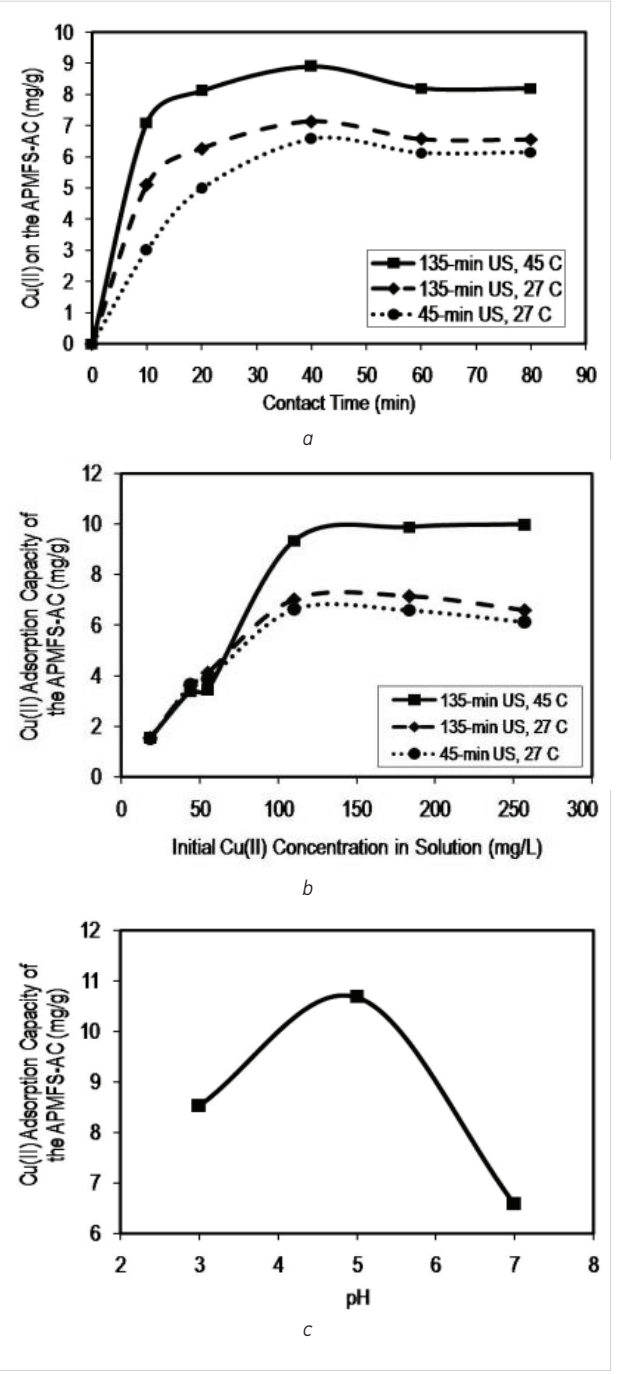

Effect of pH on the *q*

The maximum *q* was obtained at the pH being less than 7 of Cu(II) aqueous solution (Demirbas et al., 2009; Bouhamed et al., 2012; Runtti et al., 2014; Zein et al., 2014; Gupta and Gogate, 2016). *Fig. 3(c)* shows the effect of

pH on the q of the APMFS-AC with the 135-min sonication. The adsorption test was set at the C_0 of 257.213 mg/L and 45°C. As can be seen in *Fig. 3(c)*, the trend of q over pH in the range of 2–7 was typically the same as the trend with the other heavy metal adsorption using treated APMFS powder (non-carbon and without ultrasound) in a previous study (Zein et al., 2014). However, the maximum q of the APMFS-AC was 10.68 mg/g reached at pH 5, which was the same pH for adsorption of Cu(II) by activated water melon (Gupta and Gogate, 2016) and biomass residue (Runtti et al., 2014). The q of the APMFS-AC (10.68 mg/g) in the present study was much higher than the q of treated APMFS powder (0.28 mg/g, 0.58 mg/g and 0.43 mg/g for Cr(III), Zn(II) and Cd(II), respectively) (Zein et al., 2014).

It can be expected from electrostatic force of attraction that increasing pH from 2 to 5 increased the amount of Cu(II) on the APMFS-AC active sites of ketones, carboxylic acids and amides. The conjugate was based on the presence of non-hydrogen bonded O–H stretching in the FT-IR analysis. The trend was reasonable because of decreasing protons of H^+ on the active sites to compete with Cu(II) (Mi-Hwa et al., 2010; Zein et al., 2014). On the other hand, decreasing the q of the APMFS-AC to 6.58 mg/g at pH 7 could be due to the copper complex formation on the APMFS-AC (Cordero et al., 2004).

Effect of sonication time and temperature on Cu(II) adsorption isotherm

The maximum q of the APMFS-AC was obtained using the Langmuir equation (Langmuir, 1981), where the linearized form (Zengin et al., 2012) is:

$$\frac{C_e}{q_e} = \frac{1}{q_m K_L} + \frac{1}{q_m} C_e \quad (1)$$

Where C_e (mg/L) is the solution phase Cu(II) concentration at t_e; q_e (mg/g) is the equilibrium adsorption capacity; q_m (mg/g) represents the Langmuir mono-layer q; and K_L (L/mg) represents the pores volume of Langmuir.

The values of K_L and q_m were calculated using the slope intercept of the trend line shown in *Fig. 4(a)*. The nature and type of an adsorption isotherm can be obtained where $R_L = 1/(1 + K_L C_o)$ for the highest C_0. The R_L values $R_L = 0$, $R_L > 0$, $R_L = 1$, $0 < R_L < 1$ (Karagoz et al., 2008) represent the adsorption being irreversible, unfavourable, linear or favourable, respectively. The Freundlich equation (Freundlich, 1960), and the linearized form (Silverstein et al., 1981) are expressed as:

$$\log q_e = \frac{1}{n} \log C_e + \log K_F \quad (2)$$

Where K_F (L/mg) is the pore volume based on Freundlich; and $1/n$ denotes the adsorption intensity.

The values of these parameters can be obtained with the intercept and slope of the trend line shown in *Fig. 4(b)*.

As shown in *Fig. 4*, the Langmuir model provided the best fit with the R^2 being 0.993 and 0.993 for the APMFS-AC 45-min sonication and APMFS-AC 135-min sonication, respectively, at 27°C, and it was 0.943 for the APMFS-AC 135-min sonication at 45°C. As expected in the previ-

Fig. 4. *Adsorption isotherm models of (a) Langmuir and (b) Freundlich for Cu(II) adsorption of the APMFS-AC. Experimental condition: the C_0 of 18.372–257.213 mg/L at a 60-min contact time and pH 5*

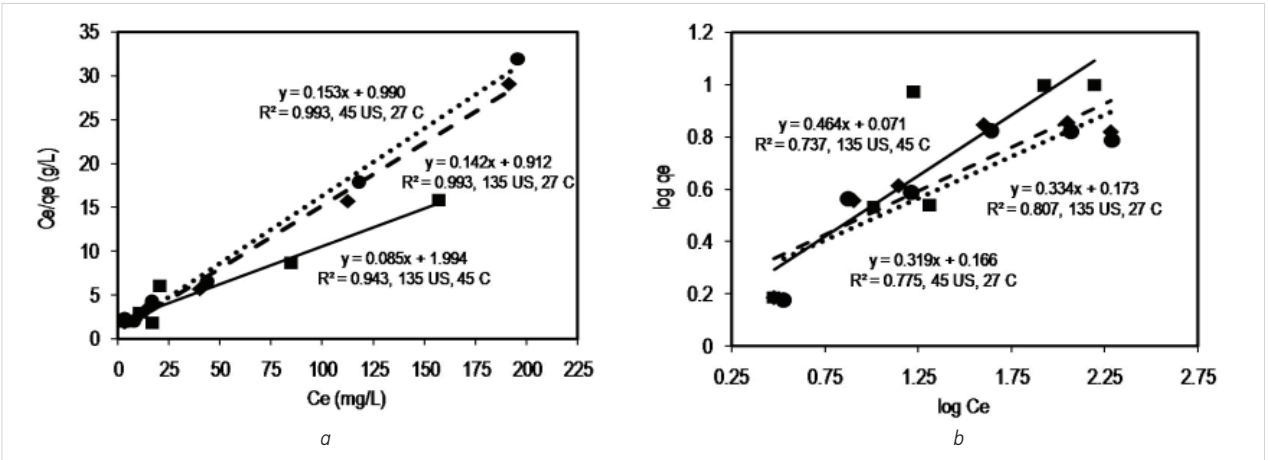

ous discussion, each active site of the APMFS-AC should adsorb only one ion of Cu(II) to form a monolayer on the APMFS-AC surface. The Langmuir mono-layer adsorption capacity (q_m) obtained was 6.535 mg/g, 7.042 mg/g and 11.765 mg/g for the APMFS-AC 45 US, 27°C, the APMFS-AC 135 US, 27°C and the APMFS-AC 135 US, 45°C, respectively. Meanwhile, using the Langmuir constant (K_L) 0.154 L/mg, 0.156 L/mg and 0.0426 L/mg, the R_L obtained was 0.0245, 0.024 and 0.084, respectively, confirming that it was favourable adsorption. Overall, the sonication time of the APMFS-AC affected the Langmuir-based q whereas increasing the sonication time from 45 min to 135 min increased the Langmuir-based q by 7.758%. The temperature affected the q of the APMFS-AC with the 135-min sonication, and the rising adsorption temperature from 27°C to 45°C lifted it up by 67.069%. In addition, the Langmuir models confirmed that a single layer on the activated carbon should correspond to a pseudo second order model (Rajamohan et al., 2023).

Effect of sonication time and temperature on total pore volume and saturation capacity

The total pore volume (C_{BET}) and the saturation capacity (q_s) were determined using the BET model (Foo and Hameed, 2010):

$$\frac{C_e}{q_e\,(C_s - C_e)} = \frac{1}{q_s C_{BET}} + \frac{(C_{BET} - 1)}{q_s C_{BET}}\left(\frac{C_e}{C_s}\right) \quad (3)$$

From a linear plot $\frac{C_e}{q_e(C_s - C_e)}$ vs $\frac{C_e}{C_s}$, the C_{BET} and q_s can be calculated from the slope and the intercept. Because C_{BET} and $C_{BET}(C_e/C_s)$ have a value greater than 1, *Equation* (*3*) can be simplified into:

$$q_e = \frac{q_s}{1 - \left(\frac{C_e}{C_s}\right)} \quad (4)$$

This model is extended to the liquid-solid interface and is described in a non-linear form as follows:

$$q_e = \frac{q_s C_{BET} C_e}{(C_s - C_e)\left[1 + (C_{BET} - 1)\left(\frac{C_e}{C_s}\right)\right]} \quad (5)$$

Where C_{BET} (L/mg) and q_s (g/mg) are the total pore volume and the saturation capacity, respectively.

The value of C_{BET} (L/mg) and q_s (g/mg) can be obtained using an optimization approach in the Microsoft® Excel software (the add-in solver tool) by minimizing the sum of squared errors (SSE) between the experimental data and the theoretical data predicted (Karri et al., 2017). The plots of the BET non-linear isotherm model are shown in *Fig. 5*.

Fig. 5. *The BET model plots for Cu(II) adsorption of the APMFS-AC. Experimental condition: the C_0 of 18.372–257.213 mg/L at a 60-min contact time and pH 5*

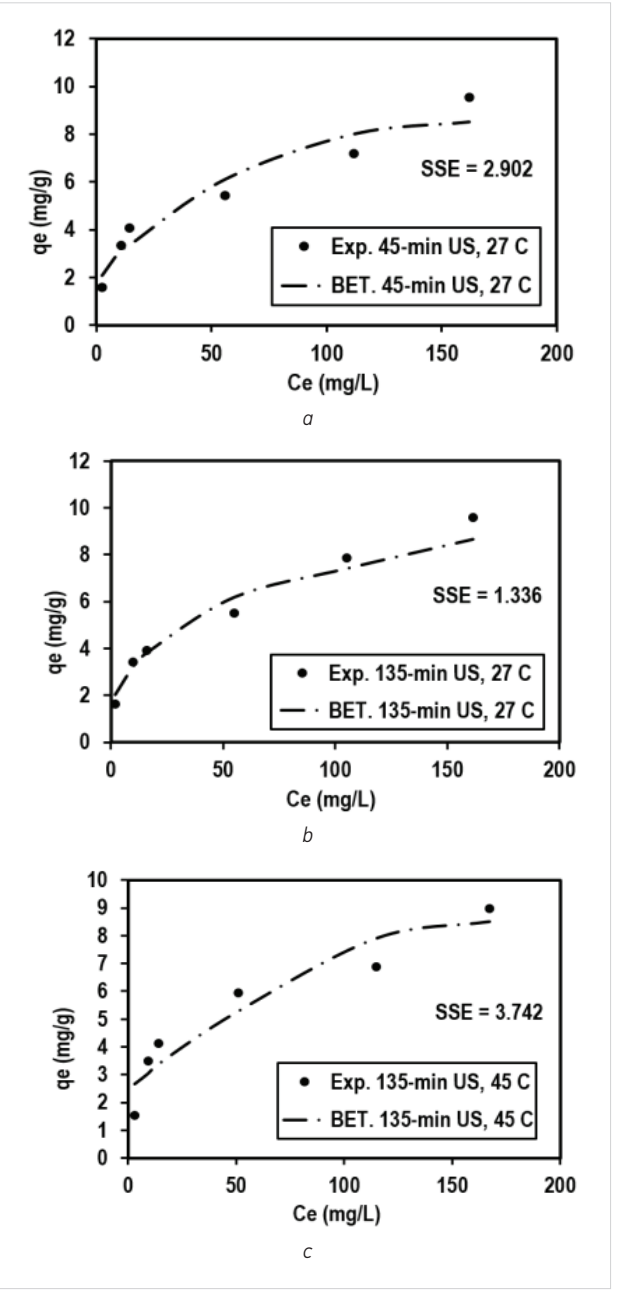

The C_{BET} for the APMFS-AC 45 US, 27°C, the APMFS-AC 135 US, 27°C, and the APMFS-AC 135 US, 45°C, obtained were 3.403 L/mg, 3.445 L/mg, and 3.987 L/mg, respectively. Meanwhile, the q_s for the APMFS-AC 45 US, 27°C, the APMFS-AC 135 US, 27°C, and the APMFS-AC 135 US, 45°C, obtained were 7.579 mg/g, 8.944 mg/g, and 13.029 mg/g, respectively. The BET results also showed clearly the effect of the sonication time on the total pore volume and the saturation capacity whereas increasing the sonication time from 45 min to 135 min increased the *CBET* value from 3.403 mg/g to 3.445 mg/g, respectively. The increase in the sonication time inclined the q_s value from 7.579 mg/g to 8.944 mg/g. Temperature also affected these parameters where increasing the adsorption temperature from 27°C to 45°C lifted the q_s by 45.674%, and increased the C_{BET} by 15.704%. In addition, the more saturation capacity should be caused by the higher BET (Wang et al., 2021).

Effect of sonication time and adsorption temperature on Cu (II) adsorption kinetics

To know the effect of sonication time and temperature of adsorption, the linearized form of the pseudo first-order kinetics (PFOK) model by Lagergren (Lagergren, 1989), given as *Equation* (*6*), and the linearized form of the pseudo second-order kinetics (PSOK) model (Ho et al., 1996), given as *Equation* (*7*), were used, and the results were plotted in *Figs. 6(a)* and *(b)*, respectively:

$$\log(q_e - q_t) = \log q_e - \left(\frac{k_L t}{2.303}\right) \quad (6)$$

$$\frac{t}{q_t} = \frac{1}{k_H q_e^2} + \frac{t}{q_e} \quad (7)$$

Where: q_t (mg/g) represents the q of the APMFS-AC at the time of t (min); q_e (mg/g) is the equilibrium adsorption capacity; k_L (/min) denotes the rate constant of the PFOK model; and k_H (g/mg.min) represents the rate constant of the PSOK model.

The data presented in *Fig. 3(a)* were taken to plot *Figs. 6(a)* and *(b)* showing that the PSOK model gave the best fit indicated by the R^2 values. It means that chemisorption played an important role where only one layer of molecules of Cu(II) mostly formed. This result was in line with the Langmuir adsorption isotherms (Sarojini et al., 2018; Rajamohan et al., 2023). The effect of the sonication time and the adsorption temperature on the adsorption kinetics was highlighted in *Fig. (6)*. The q of the APMFS-AC for the sonication time of 45 min and 135 min at 27°C was almost the same, which was 6.849 to 6.896 mg/g, respectively. It improved to 8.475 mg/g at 45°C when using the APMFS-AC with the 135-min sonication. Meanwhile, the adsorption rate onto the APMFS-AC increased from to 0.161 g/mg.min to 0.336 g/mg.min as a result of raising the sonication time from 45 min to 135 min at 27°C, and it increased to 0.473 g/mg.min at 45°C when using the APMFS-AC with the 135-min sonication. Overall, the longer the sonication time and the higher the adsorption temperature, the faster the Cu(II) adsorption onto the APMFS-AC was achieved.

Fig. 6. *Adsorption kinetics models of (a) pseudo first-order and (b) pseudo second order for Cu(II) adsorption of the APMFS-AC. Experimental condition: The C_0 of 257.213 mg/L at pH 5*

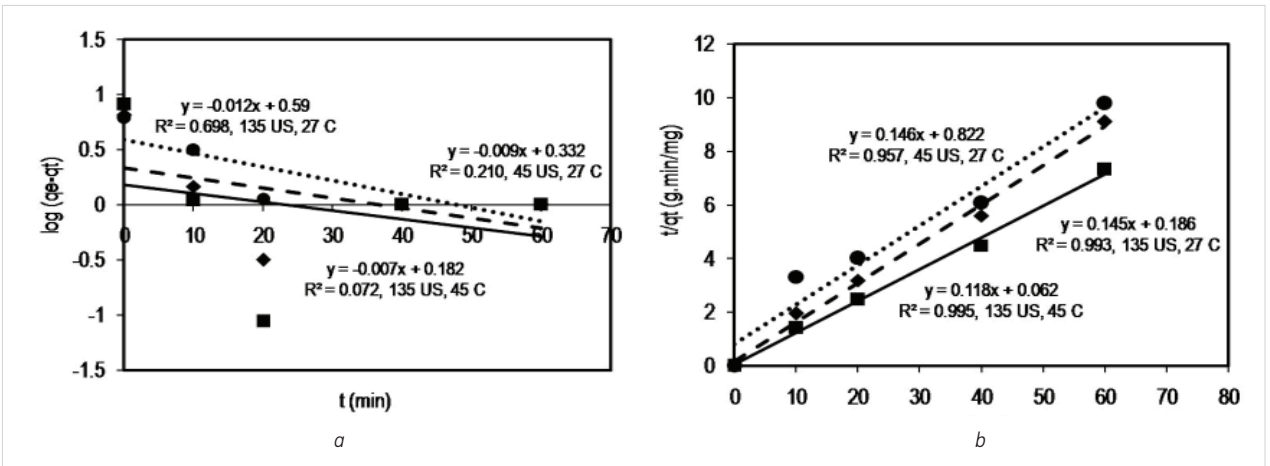

Cu(II) adsorption thermodynamics

Thermodynamic equations were used to determine the change of enthalpy, the change of free energy and the change of entropy for Cu(II) adsorption onto the APMFS-AC. The change of enthalpy was worked out using *Equation* (*8*) of the van't Hoff linear model (Mengistie et al., 2008):

$$\ln K_d = \frac{\Delta S}{R} - \frac{\Delta H^0}{RT} \quad (8)$$

Where: ΔH^0 (J/mol) is the change of enthalpy at T (K); K_d (L/mg) is defined as q_e/C_e) where q_e and C_e are at the maximum C_0 of the Langmuir plot; and R (8.314 J/mol K) is the ideal gas constant.

The values of thermodynamic parameters C_{e1}, C_{e2}, q_{e1}, q_{e2}, K_{d1}, K_{d2}, T_1, T_2 were taken from the Langmuir adsorption isotherm data presented in *Fig. 4(a)*, 191.406 mg/L, 157.368 mg/L, 6.581 mg/g, 9.985 mg/g, 0.034 L/g, 0.063 L/g, 300.15 K and 318.15 K, respectively. C_{e1} and C_{e2} represent the C_e at T_1 and T_2, respectively, as well as the notation of q_{e1} and q_{e2}, K_{d1} and K_{d2} represent the q and K_d at the T_1 and T_2, respectively. An additional experiment of adsorption isotherms was conducted at 309.15 K (T_3), and the values of C_{e3}, q_{e3}, K_{d3} and T_3 obtained were 176.001 mg/g, 8.293 mg/g and 0.047 L/g, respectively, and Langmuir q obtained was 9.171 mg/g. As a result, the trend line of $\ln k_d = 7.46–3250.53/T$ was obtained, and ΔH^0 of 27.035 kJ/mol was obtained. The positive value of ΔH^0 indicates the endothermic nature of the adsorption. It is reasonable because the entropy increases when the adsorbate is being adsorbed, leading to a positive sign of enthalpy as a driving force of adsorption (Papirer, 2000; Kumar and Awasthi, 2009). The increasing T from 300.15 K to 318.15 K caused the increase in the q from 7.042 mg/g to 11.765 mg/g. It was reasonable according to the Le Chatelier principle (Rao, 2004), and the activation energy should be in a positive sign (Tan et al., 2009). The activation energy can be obtained using *Equation* (*9*):

$$\ln q_m = q_m - \frac{E}{R}\left(\frac{1}{T}\right) \quad (9)$$

Where: q_m (mg/g) represents the q based on Langmuir at T (K) (Rao 2004).

As a result, the trend line form obtained for the q_{m1}, q_{m2}, q_{m3}, T_1, T_2 and T_3 being 7.042 mg/g, 11.765 mg/g, 9.171 mg/g, 300.15 K, 318.15 K and 309.15 K, respectively, was ln q_m = 11.02–2722.80/T, and the activation energy E obtained was 22.637 kJ/mol. The E positive sign indicated that chemisorption was taking place, and it refers to the Langmuir monolayer adsorption (Worch, 2012).

The change of entropy ΔS^0 (J/mol.K) can be determined using *Equation* (*8*) which was solved to be ln k_d = 7.46–3250.53/T, and it was 0.062 kJ/mol.K. The positive sign of ΔS^0 value is for an increase in the degree of freedom of adsorption (Papirer, 2000; Kumar and Awasthi, 2009). Meanwhile, change of free energy ΔG^0 (J/mol) can be obtained using *Equation* (*10*) (Lahreche et al., 2022), respectively:

$$\Delta G^0 = \Delta H^0 - T\Delta S^0 \quad (10)$$

The ΔG^0 values obtained using *Equation* (*10*), ΔS^0 being 0.062 kJ/mol.K and ΔH^0 being 27.035 kJ/mol, were 8.409 kJ/mol and 7.292 kJ/mol for the T of 300.15 K and 318.15 K, respectively. The positive sign of ΔS^0 and ΔH^0, and the negative sign of ΔG indicated a spontaneous process and endothermic nature (Benchikh et al., 2022), which equires an external energy source to increase the Cu(II) adsorption capacity.

Conclusions

Activating carbon from APMFS waste using 0.5 M KOH with the assistance of ultrasound allowed restructuring the active binding sites and produced more pores including transport pores in the APMFS-AC. The results were confirmed by the FT-IR and SEM analyses. Cu(II) adsorption isotherms correlated well with the Langmuir model, and raising the sonication time from 45 min to 135 min increased the q at 27°C from 6.535 mg/g to 7.042 mg/g, respectively. Increasing the adsorption temperature from 27°C to 45°C improved the q from 7.042 mg/g to 11.765 mg/g, respectively, using the APMFS-AC with the 135-min sonication. The BET saturation capacity and the total pore volume obtained were 13.029 mg/g and 3.987 L/mg, respectively. The kinetics study showed that Cu(II) adsorption at 27°C followed the PSOK model. The adsorption rate increased from to 0.161 g/mg.min to 0.336 g/mg.min as a result of raising the sonication time, and it increased to

0.473 g/mg.min at 45°C using the APMFS-AC with the 135-min sonication. The *q* at 27°C and pH 5 was 10.68 mg/g. The thermodynamic study resulted in the values of enthalpy, free energy and entropy changes, and activation energy, indicating that the Cu(II) adsorption onto the APMFS-AC should be endothermic, chemical adsorption, increasing the degree of freedom, and spontaneous adsorption.

Acknowledgments

The authors would like to appreciate Universitas Syiah Kuala for technical support in the adsorption experiment and FT-IR analyses at Chemical Engineering Department, SEM analyses at Mechanical Engineering Department, and AAS analyses at Mathematics and Science Faculty.

References

Bala M., Shehu R.A. and Lawal M. (2008) Determination of the level of some heavy metals in water collected from two pollution - Prone irrigation areas around Kano Metropolis. Bayero Journal of Pure and Applied Sciences 1(1): 6-38. https://doi.org/10.4314/bajopas.v1i1.57511

Benchikh I., Dahou F.Z., Lahreche S., Sabantina L., Benmimoun Y. and Benyouce A. (2022) Development and characterisation of novel hybrid materials of modified ZnO-SiO2 and polyaniline for adsorption of organic dyes. International Journal of Environmental Analytical Chemistry. Available at: https://www.tandfonline.com/doi/abs/10.1080/03067319.2022.2107921 (accessed 10 July 2022). https://doi.org/10.1080/03067319.2022.2107921

Bouhamed F., Elouear Z. and Bouzid, J. (2012) Adsorptive removal of copper(II) from aqueous solutions on activated carbon prepared from Tunisian date stones: Equilibrium, kinetics and thermodynamics. Journal of the Taiwan Institute of Chemical Engineers 43(5): 741-749. https://doi.org/10.1016/j.jtice.2012.02.011

Carl L.K., Harry J.M. and Elizabeth M.W. (2003) A review: The impact of copper on human health, International Copper Association Ltd., New York.

Chakravarty P., Sarma N. S. and Sarma H.P. (2010) Removal of lead(II) from aqueous solution using heartwood of Areca catechu powder. Desalination 256, 16-21. https://doi.org/10.1016/j.desal.2010.02.029

Chen C.J., Wei L.B., Zhao P.C., Li Y., Hu H.Y. and Qin Y.B. (2011) Study on preparation of activated carbon from corncob furfural residue with ZnCl2 by microwave irradiation. New Materials and Advanced Materials 152-153(1-2): 1322-1327. https://doi.org/10.4028/www.scientific.net/AMR.152-153.1322

Cordero B., Lodeiro P., Herrero R. and Sastre de Vicente M.E. (2004) Biosorption of Cadmium by Fucus spiralis. Environmental Chemistry 1, 180-187. https://doi.org/10.1071/EN04039

Commenges-Bernole N. and Marguerie J. (2009) Adsorption of heavy metals on sonicated activated sludge. Ultrasonics Sonochemistry 16(1): 83-87. https://doi.org/10.1016/j.ultsonch.2008.05.006

Dehdashti A., Khavanin A., Rezaee A. and Asilian H. (2010) Regeneration of granular activated carbon saturated with gaseous toluene by microwave irradiation. Journal of Engineering Environmental Science 34, 49-58.

Demirbas E., Dizge N., Sulak M.T. and Kobya M. (2009) Adsorption kinetics and equilibrium of copper from aqueous solutions using hazelnut shell activated carbon. Chemical Engineering Journal 148(2-3): 480-487. https://doi.org/10.1016/j.cej.2008.09.027

Dimple L. (2014) Adsorption of heavy metals: A review. International Journal of Environmental Research and Development 4(1): 41-48.

Foo, K.Y., Hameed, B.H. (2010) Insights into the modeling of adsorption isotherm systems. Chemical Engineering Journal, 156: 2-10. https://doi.org/10.1016/j.cej.2009.09.013

Freundlich H. (1960) Adsorption in solution. The Journal of Physical Chemistry 57, 384-410.

Gupta H. and Gogate P.R. (2016) Intensified removal of copper from waste water using activated water melon based biosorbent in the presence of ultrasound. Ultrasonics Sonochemistry 30: 113-122. https://doi.org/10.1016/j.ultsonch.2015.11.016

Hesas R.H., Daud W. M. A., Sahu J.N. and Arami-Niya A. (2013) The effects of a microwave heating method on the production of activated carbon from agricultural waste: A review. Journal of Analytical and Applied Pyrolysis 100: 1-11. https://doi.org/10.1016/j.jaap.2012.12.019

Ho Y.S., Wase D.A.J. and Forster C.F. (1996) Kinetic studies of competitive heavy metal adsorption by sphagnum moss peat. Environmental Technology 17: 71-77. https://doi.org/10.1080/09593331708616362

Imamoglu M. and Tekir O. (2008) Removal of copper (II) and lead (II) ions from aqueous solutions by adsorption on activated carbon from a new precursor hazelnut husks. Desalination 228(1-3): 108-113. https://doi.org/10.1016/j.desal.2007.08.011

Ishak M.R., Sapuan S.M., Leman Z., Rahman M.Z.A., Anwar U.M.K. and Siregar J.P. (2013) Sugar palm (Arenga pinnata), Its fibres, polymers and composites. Carbohydrate Polymers 91(2): 699-710. https://doi.org/10.1016/j.carbpol.2012.07.073

Karagoz S., Tay T., Ucar S. and Erdem M. (2008) Activated carbons from waste biomass by sulfuric acid activation and their

use on methylene blue adsorption. Bioresource Technology 99: 6214-6222. https://doi.org/10.1016/j.biortech.2007.12.019

Karri, R.R., Sahu, J.N., Jayakumar, N.S. (2017) Optimal isotherm parameters for phenol adsorption from aqueous solutions onto coconut shell based activated carbon: Error analysis of linear and non-linear methods. Journal of the Taiwan Institute of Chemical Engineers, 80: 472-487. https://doi.org/10.1016/j.jtice.2017.08.004

Klasson K.T., Wartelle L.H., James E., Rodgers J.E. and Lima, I.M. (2009) Copper(II) adsorption by activated carbons from pecan shells: Effect of oxygen level during activation. Industrial Crops and Products 30(1): 72-77. https://doi.org/10.1016/j.indcrop.2009.01.007

Kumar A. and Awasthi A. (2009) Bioseparation engineering, I.K. International Publishing House, Pvt. Ltd., New Dehli, India.

Kurniawan T.A.G., Chan Y.S., Lo, W. and Babel S. (2006) Comparisons of low-cost adsorbents for treating waste waters laden with heavy metals. Science of the Total Environment 366(2-3): 409-426. https://doi.org/10.1016/j.scitotenv.2005.10.001

Lagergren S. (1989) About the theory of so-called adsorption of soluble substances. Kungliga Svenska Vetenskapsakademies Handlingar 24(4): 1-39.

Lahreche S., Moulefera I., El Kebir A., Sabantina L., Kaid M. and Benyoucef A. (2022) Application of Activated Carbon Adsorbents Prepared from Prickly Pear Fruit Seeds and a Conductive Polymer Matrix to Remove Congo Red from Aqueous Solutions. Fibers 10(1): 7. https://doi.org/10.3390/fib10010007

Langmuir I. (1981) The adsorption of gases on plane surface of glass, mica and platinum. Journal of the American Chemical Society40(9): 1361-1403. https://doi.org/10.1021/ja02242a004

Largitte L. and Lodewyckx P. (2014) Studying different methods to determine the thermo kinetic constants in the adsorption of Pb2+ on an activated carbon from Bois carré seeds. Journal of Environmental Chemical Engineering 2(2): 788-795. https://doi.org/10.1016/j.jece.2014.02.001

Liu X., Zhang W. and Zhang, Z. (2014) Preparation and characteristics of activated carbon from waste fiberboard and its use for adsorption of Cu(II). Materials Letters 116: 304-306. https://doi.org/10.1016/j.matlet.2013.11.062

Marlina, Iqhrammullah M., Saleha S., Fathurrahmi, Maulina, F.P. and Idroes, R. (2020) Polyurethane film prepared from ball-milled algal polyol particle and activated carbon filler for NH3-N removal. Heliyon 6(8): e04590. https://doi.org/10.1016/j.heliyon.2020.e04590

Medhi H., Chowdhury P.R., Baruah P.D., and Bhattacharyya K.G. (2020) Kinetics of Aqueous Cu(II) Biosorption onto Thevetia peruviana Leaf Powder. ACS Omega 5: 13489-13502. https://doi.org/10.1021/acsomega.9b04032

Mengistie A.A., Siva R.T., Prasada R.A.V. and Singanan, M. (2008) Removal of lead(II) ions from aqueous solutions using activated carbon from Militia ferruginea plant leaves. Bulletin of the Chemical Society of Ethiopia 22(3): 349-360. https://doi.org/10.4314/bcse.v22i3.61207

Milenković D.D., Bojić A.L.J. and Veljković V.B. (2013) Ultrasound-assisted adsorption of 4-dodecylbenzene sulfonate from aqueous solutions by corn cob activated carbon. Ultrasonics Sonochemistry 20(3): 955-962. https://doi.org/10.1016/j.ultsonch.2012.10.016

Minamisawa M., Minamisawa H., Yoshida S. and Takai, N. (2004) Adsorption behavior of heavy metals on biomaterials. Journal of Agricultural and Food Chemistry 52(18): 5606-5615. https://doi.org/10.1021/jf0496402

Moreno-Pirajan J.C. and Giraldo L. (2010) Adsorption of copper from aqueous solution by activated carbons obtained by pyrolysis of cassava peel. Journal of Analytical and Applied Pyrolysis 87(2): 188-193. https://doi.org/10.1016/j.jaap.2009.12.004

Mordor Intelligence (2022) Activated Carbon Market - Growth, Trends, Covid-19 Impact, and Forecasts (2022 - 2027). Available at: https://www.reportlinker.com/p06360546/Activated-Carbon-Fiber-Market-Growth-Trends-COVID-19-Impact-and-Forecasts.html (accessed 12 July 2022).

Muslim A. (2017) Australian Pine Cones-Based Activated Carbon for Adsorption of Copper in Aqueous Solution. Journal of Engineering Science and Technology 12(2): 280-295.

Muslim A., Purnawan E., Nasrullah, Meilina H., Azwar M.Y., Deri N.O., Kadri A. (2022) Adsorption of copper ions onto rice husk activated carbon prepared using ultrasound assistance: optimization based on step-by-step single variable knockout technique. Journal of Engineering Science and Technology (JESTEC) 17(4): 2496-2511.

Muslim A., Zulfian, Ismayanda H., Devrina E. and Fahmi H. (2015) Adsorption of Cu(II) from the aqueous solution by chemical activated adsorbent of areca catechu shell. Journal of Engineering Science and Technology 10(12): 1654-1665.

Pandian A.M.K., Gopalakrishnan B., Rajasimman M., Rajamohan N. and Karthikeyan C. (2021) Green synthesis of bio-functionalized nano-particles for the application of copper removal - characterization and modeling studies. Environmental Research 197: 111140. https://doi.org/10.1016/j.envres.2021.111140

Papirer, E. (2000) Adsorption on silica surfaces: Surfactant science series. Marcel Dekker, Inc., New York, USA. https://doi.org/10.1201/9781482269703

Rao S. R. (2004) Surface Chemistry of froth flotation: Volume 1: Fundamentals. Springer Science, New York, USA. https://doi.org/10.1007/978-1-4419-9124-9_1

Rajamohan N., Bosu S., Rajasimman M., Varjani S. (2023) Environmental remediation of selenium using surface modified carbon nano tubes - Characterization, influence of variables, equilib-

rium and kinetic analysis. Environmental Research 216: 114629. https://doi.org/10.1016/j.envres.2022.114629

Rajamohan N., Bosu S., Ngo G.H. and Al-Shibli N. (2022) Fabrication of modified carbon nano tubes based composite using ionic liquid for phenol removal. Molecular Catalysis 533, 112792. https://doi.org/10.1016/j.mcat.2022.112792

Runtti H., Tuomikoski S., Kangas T., Lassi U., Kuokkanen T. and Rämö, J. (2014) Chemically activated carbon residue from biomass gasification as a sorbent for iron(II), copper(II) and nickel(II) ions. Journal of Water Process Engineering 4, 12-24. https://doi.org/10.1016/j.jwpe.2014.08.009

Silverstein R.M., Bassler G.C. and Morrill T.C. (1981) Spectrometric Identification of Organic Compounds, 4th ed., John Wiley and Sons, New York.

Srivastava N.K. and Majumder B.C. (2008) Novel biofiltration methods for the treatment of heavy metals from industrial waste water. Journal of Hazardous Materials 151(1): 1-8. https://doi.org/10.1016/j.jhazmat.2007.09.101

Tan I.A.W., Ahmad A.L. and Hameed B.H. (2009) Adsorption isotherms, kinetics, thermodynamics and desorption studies of 2,4,6-trichlorophenol on oil palm empty fruit bunch-based activated carbon. Journal of Hazardous Materials 164(2-3): 473-482. https://doi.org/10.1016/j.jhazmat.2008.08.025

Theophanides T. and Anastassopoulou J. (2002) Copper and carcinogenesis. Critical Reviews in Oncology/Hematology 42(1): 57-64. https://doi.org/10.1016/S1040-8428(02)00007-0

Tseng R.L. and Tseng S.K. (2005) Pore structure and adsorption performance of the KOH-activated carbons prepared from corncob. Journal of Colloid and Interface Science 287(2): 428-437. https://doi.org/10.1016/j.jcis.2005.02.033

Wang, P., Ding, F., Huang, Z., Fu, Z., Zhao, P., Shuhui Men, S. (2021) Adsorption behavior and mechanism of Cd (II) by modified coal-based humin. Environmental Technology and Innovation, 23, 101699. https://doi.org/10.1016/j.eti.2021.101699

Wong K.K., Lee C.K., Low K.S. and Haron M.J. (2003) Removal of Cu and Pb by tartaric acid modified rice husk from aqueous solutions. Chemosphere 50, 23-28. https://doi.org/10.1016/S0045-6535(02)00598-2

Worch E. (2012) Adsorption technology in water treatment: Fundamentals, processes, and modeling, Walter de Gruyter, Berlin. https://doi.org/10.1515/9783110240238

Yan-Biao G., Hong F., Chong C., Chong-Jian J., Fan X., and Ying L. (2013) Heavy metal concentrations in soil and agricultural products near an industrial district. Polish Journal of Environmental Studies 22(5): 1357-1362.

Yang T. and Lua A. (2003) Characteristics of activated carbons prepared from pistachio-nut shells by physical activation. Journal of Colloid and Interface Science 267(2): 408-417. https://doi.org/10.1016/S0021-9797(03)00689-1

Zein R., Hidayat D.A., Elfia M., Nazarudin N. and Munaf E. (2014) Sugar palm Arenga pinnata Merr (Magnoliophta) fruit shell as biomaterial to remove Cr(III), Cr(VI), Cd(II) and Zn(II) from aqueous solution. Journal of Water Supply: Research and Technonoly-AQUA 63(7): 553-559. https://doi.org/10.2166/aqua.2014.120

Zengin A., Akalin M.K., Tekin K., Erdem M., Turga T. and Karagoz K. (2012) Preparation and Characterization of Activated Carbons from Waste Melamine Coated Chipboard by KOH Activation. Ekoloji 21(85): 123-128. https://doi.org/10.5053/ekoloji.2012.8514